

## Bismuth Silicate/Silica-Titania Synthesis from In Situ Decomposition of Oil Palm Leaves as Silica Source

Salprima Yudha S<sup>1,2\*</sup>, Morina Adfa<sup>1,2</sup>, Swadexi Istiqphara<sup>3</sup>, Muhamad Alvin Reagen<sup>1</sup>

<sup>1</sup>Department of Chemistry, Faculty of Mathematics and Natural Sciences, Universitas Bengkulu, Bengkulu, 38122, Indonesia

<sup>2</sup>Research Center of Sumatera Natural Products and Functional Materials, Universitas Bengkulu, Bengkulu, 38122, Indonesia

<sup>3</sup>Department of Electrical Engineering, Faculty of Engineering, Institut Teknologi Sumatera, Lampung Selatan, 35365, Indonesia

\*Corresponding author: sp.yudha.s@gmail.com; salprima@unib.ac.id

### Abstract

In this work, bismuth silicate-titania has been synthesized in two stages by utilizing bismuth oxynitrate as an elemental source of bismuth, oil palm leaves (OPL) as a source of silica and titanium tetraisopropoxide (TTIP) as source of titania (TiO<sub>2</sub>). In the first stage, bismuth silicate/silica (Bi<sub>4</sub>Si<sub>3</sub>O<sub>12</sub>/SiO<sub>2</sub>) was formed, which occurs due to the in-situ decomposition of palm leaves and reacts directly with the bismuth precursor at high temperatures (900°C). The reaction could possibly occur through a solid-state reaction mechanism between bismuth oxide and silica or through a more complex mechanism within the reaction mixture. The resulting product then reacts with TTIP, which is added and heated at the same temperature to form Bi<sub>4</sub>Si<sub>3</sub>O<sub>12</sub>/SiO<sub>2</sub>-TiO<sub>2</sub> (bismuth silicate/silica-titania). Characterization of the as-prepared product using X-ray diffraction showed the dominance of bismuth silicate and small amount of titania (TiO<sub>2</sub>). As a result, TiO<sub>2</sub> could not be detected in the diffractogram. Nevertheless, an analysis using energy-dispersive X-rays showed the presence of titanium elements in the resulting composite. The results of this study can be used to develop ternary metal oxides based on natural resources and agricultural wastes, such as oil palm leaves.

### Keywords

Bismuth Silicate, Titania, Oil Palm Leaves, Bismuth Oxynitrate, Agricultural Waste

Received: 9 March 2023, Accepted: 7 June 2023

<https://doi.org/10.26554/sti.2023.8.3.397-402>

## 1. INTRODUCTION

Binary and ternary metal oxide structures have vast technological uses, e.g., transistors and computing, devices and are of basic scientific interest because of their electrical, optical, and catalytic properties. Extensive research has been conducted in the past few years to create novel synthetic techniques for these materials (Mao et al., 2005; Bilecka et al., 2008; Wang and Wu, 2017). For instance, to form multilayered thin films demonstrating superhydrophilicity, antifogging ability in the dark environment, and self-cleaning ability toward stearic acid under photocatalytic conditions, a mesoporous SiO<sub>2</sub>/Bi<sub>2</sub>O<sub>3</sub>/TiO<sub>2</sub> compound was synthesized using a sol-gel method (Bai et al., 2017). Another SiO<sub>2</sub>/Bi<sub>2</sub>O<sub>3</sub>/TiO<sub>2</sub> compound, which was prepared using Bi(NO<sub>3</sub>)<sub>3</sub>, SiO<sub>2</sub>, and TiOSO<sub>4</sub> under mild conditions, exhibited good photocatalytic performance toward benzene degradation (Ren et al., 2015). To afford an effective electrode material with a discharging capacity of 298 mAh g<sup>-1</sup>, TiO<sub>2</sub>/SiO<sub>2</sub> hybrid material with a TiO<sub>2</sub>:SiO<sub>2</sub> molar ratio of 8:20 was doped with Bi<sub>2</sub>O<sub>3</sub> (2% mass) and calcined at 800°C (Kurc et al., 2018). Bi<sub>2</sub>O<sub>3</sub>/TiO<sub>2</sub>/SiO<sub>2</sub> with various ratios was

synthesized from their single metal oxide components at high temperatures, with glass formation occurring depending on the composition ratio (Slavov and Dimitriev, 2016). Moreover, at high temperatures, a mixture of Bi<sub>2</sub>O<sub>3</sub> and TiO<sub>2</sub> was reported to furnish bismuth-titanate ceramic materials (Thiruramanathan et al., 2016; Khodadoost et al., 2017; Gadea et al., 2018; Marela et al., 2021), whose insertion into mesoporous SiO<sub>2</sub> produced a material with specific characteristics for application in the catalytic degradation of methyl orange (Zaccariello et al., 2017) and as a UV protection substance in the cosmetic formulation (Zaccariello et al., 2019).

Some preparation methods to produce combined materials of bismuth oxide and silica were also reported, including their characterization and applications. For example, melting (Lu et al., 2013; Back et al., 2020), mechanical (Belik et al., 2020), hydrothermal (Jia et al., 2017), and sintering (Bai et al., 2007) processes were developed for the purposes of reactions. Another synthetic method developed for bismuth silicate is using the hydro-/solvothermal form Bi(NO<sub>3</sub>)<sub>2</sub> and commercial silica sources (Shabalina et al., 2022). As can be extracted from the literature on bismuth silicate compounds synthesis, the pres-

ence of  $\text{SiO}_2$  is very important. Generally, the silica source used in various reactions for the synthesis of bismuth silicate is a commercial precursor. The development of bismuth silicate synthesis using silica from several biomasses is still rarely reported. One recent example that has been reported is the synthesis of bismuth silicate ( $\text{Bi}_2\text{SiO}_5$ ) using silica from rice husk (Arefieva et al., 2023). The development of alternative bismuth silicate synthesis, both in terms of finding new precursors and developing methods, is an important part of chemical science. This also means that it will affect the applications that may be developed in advanced research. Therefore, the discovery of silica sources that are more sustainable and available in nature in large quantities is highly desirable. To provide information regarding the experimental utilization of abundant natural resources, especially in tropical countries, this paper describes the use of oil palm leaves (OPL) as a source of  $\text{SiO}_2$  in the context of chemical and environmental research.

## 2. EXPERIMENTAL SECTION

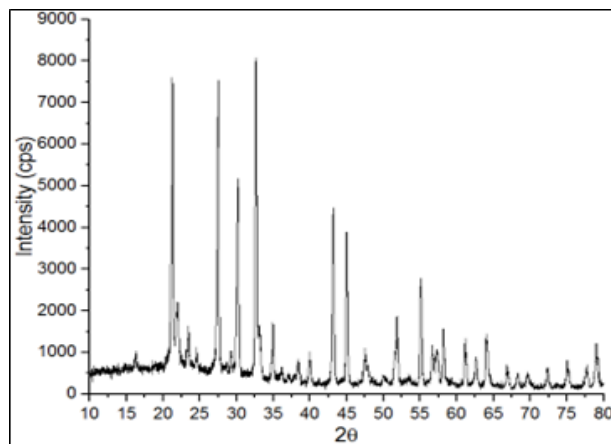
### 2.1 Materials

Bismuth oxynitrate (BON) and isopropanol (IPA) were provided by Merck, titanium tetraisopropoxide (TTIP) was purchased from Sigma-Aldrich, while  $\text{HNO}_3$  and  $\text{HCl}$  were purchased from Smart Lab Ltd. OPL used in this experiment was obtained from oil palm plantation around Bengkulu city (Indonesia). The OPL powder was treated with  $\text{HCl}$  10% under heating to remove any other minerals that may be present in the samples.

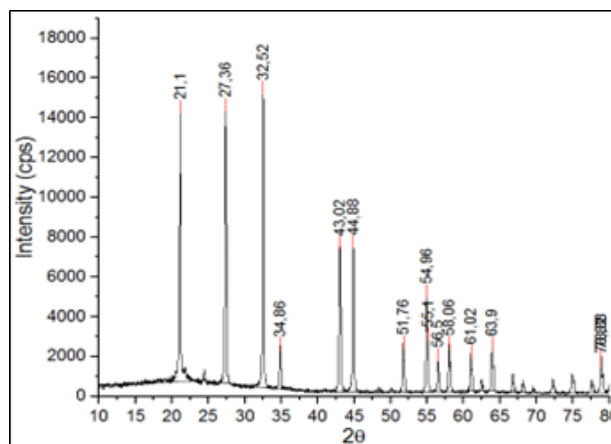
### 2.2 Methods

The first investigation is to know the possible products formed from one pot reaction of TTIP-BON and OPL powder. TTIP (0.285 g, ~0.3 mL) was diluted in 50.0 mL of IPA in a crucible. Dried OPL powder (4.0 g) was added to the TTIP solution in IPA and stirred for 30 min. Conversely, bismuth oxynitrate (BON; 1.462 g) was dissolved in  $\text{HNO}_3$  65% (10 mL) in an Erlenmeyer flask, and then, the BON solution was poured into the mixture of OPL and TTIP. The Erlenmeyer was washed with  $\text{HNO}_3$  65% twice (each with 2.5 mL) and poured again into the reaction mixture under stirring using magnetic stirring. The stirring was continued for 1 h while heating at  $85^\circ\text{C}$  until the solvents evaporated and a red-brown residue was observed. The obtained residue was kept at room temperature ( $27^\circ\text{C}$ ) for 20 h and then taken to a muffle furnace (Nabertherm, Germany). The furnace temperature was increased from room temperature to  $900^\circ\text{C}$  for 2 h, and further annealing was conducted at  $900^\circ\text{C}$  for 5 h. The procedure is modified from previously reported procedures (Batool et al., 2020; Chandrawanshi et al., 2020). The sample was cooled down to room temperature without any cooling rate control.

Based on the results using one pot reaction between OPL-TTIP and BON, a two-step reaction was performed as follows: First, 0.731 g of BON was reacted with 4.0 g of OPL as explained above but without TTIP. Then, the as-obtained



**Figure 1.** XRD Pattern of Existing Compounds in the Reaction Product of Bismuth Oxynitrate, TTIP and Oil Palm Leaves

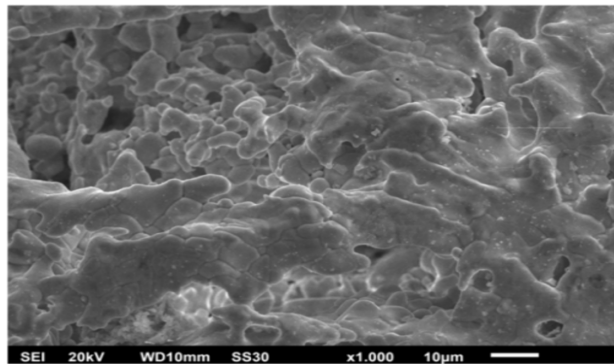
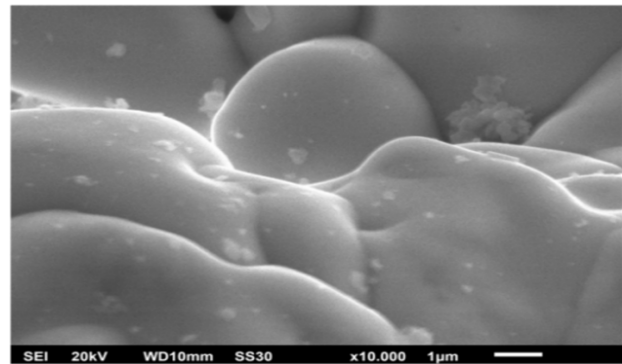


**Figure 2.** XRD Pattern of the Synthesis of Bismuth Silicate from Bismuth Oxynitrate and Oil Palm Leaves at  $900^\circ\text{C}$  for 5 h

product was mixed with TTIP in IPA, followed by solvent evaporation and calcination at  $900^\circ\text{C}$  for 5 h. The microstructure and structural properties of the synthesized powder were evaluated via X-ray diffraction (Benchtop Powder XRD Rigaku-Miniflex 600) and scanning electron microscopy (SEM). To determine the chemical composition of the nanopowder, energy-dispersive X-ray spectroscopy (EDX) (JEOL JSM 6510 LA) was used. The functional groups of bismuth silicate/silica were determined via Fourier transform infrared spectroscopy (FTIR, Bruker-Compact FT-IR Alpha II) in a wave number range of  $500\text{-}4000\text{ cm}^{-1}$ . Moreover, bismuth silicate/silica powder that has been obtained from the previous procedure, which weighed as much as 0.75 g, was then put into a crucible followed by the addition of  $\text{CHCl}_3$  as much as 20 mL. The mixture was stirred using a magnetic stirrer while adding liquid TTIP in amounts up to 1 mmol (0.284 g; 0.296 mL). Stirring was continued until the  $\text{CHCl}_3$  evaporated and left a white solid residue. The crucible containing the residue was transferred into a furnace

**Table 1.** The Remark of Existing Compounds in the Reaction Product

	Bi <sub>2</sub> O <sub>3</sub>	TiO <sub>2</sub>	Bi <sub>4</sub> Ti <sub>3</sub> O <sub>12</sub>	Bi <sub>4</sub> Si <sub>3</sub> O <sub>12</sub>
Crystallinity (%)	59.4%	39.9	70.3	70.0
Crystal Size (nm)	254	161	150	309
ICDD Card	00-041-1449	00-016-0617	00-072-1019	00-076-1729
Weight Ratio (%)	13	4	30	53

**(a)****(b)****Figure 3.** Morphology of the Binary Metal-Oxide Compound Bi<sub>4</sub>Si<sub>3</sub>O<sub>12</sub>/SiO<sub>2</sub> Resulting from Analysis using Scanning Electron Microscopy (SEM); (a) 1000× Magnification; (b) 10000×

and heated at 500°C for 3 h. The final solid obtained was analyzed via XRD and SEM-EDX.

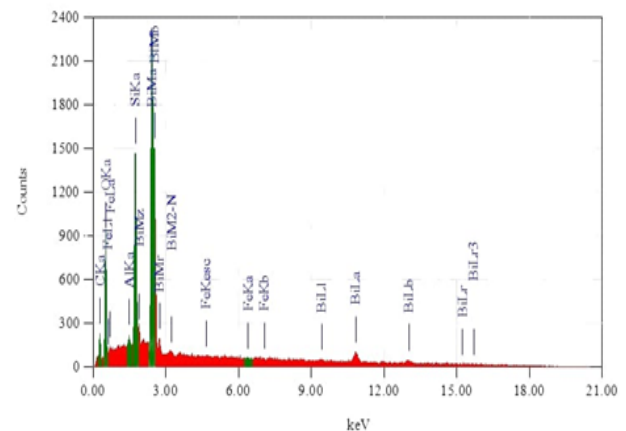
### 3. RESULTS AND DISCUSSION

XRD data are obtained based on the initial efforts that have been made by conducting in situ reactions, as shown in Figure 1. The diffractogram shows the presence of several crystalline phases that have been identified as Bi<sub>2</sub>O<sub>3</sub>, TiO<sub>2</sub>, Bi<sub>4</sub>Ti<sub>3</sub>O<sub>12</sub>, and Bi<sub>4</sub>Si<sub>3</sub>O<sub>12</sub>. Based on quantitative analysis using the existing XRD data bank, each of these oxide compounds has a weight ratio, as shown in Table 1.

Table 1 shows that bismuth precursors react more effectively with silica derived from OPL. This fact encourages researchers to first create bismuth silicate compounds before combining them with TiO<sub>2</sub> derived from TTIP. The amount of bismuth oxynitrate used was reduced in half compared to that used in the previous procedure, and the OPL was constant at 4 g. Except for the addition of TTIP, the entire procedure was the same. Figure 2 depicts the XRD results.

Figure 2 shows that several peaks (2θ) are found: 21.10°, 27.36°, 32.52°, 34.86°, 43.02°, 44.88°, 51.76°, 54.96°, 55.10°, 56.50°, 58.06°, 61.02°, 63.90°, and 78.88°. The peak at 21.10 is the peak for Bi<sub>4</sub>Si<sub>3</sub>O<sub>12</sub>, which may overlap with cristobalite silica. It is supported by other peaks that are typical peaks for Bi<sub>4</sub>Si<sub>3</sub>O<sub>12</sub>, and no peaks for Bi<sub>2</sub>O<sub>3</sub> or Bi<sub>2</sub>SiO<sub>5</sub> are detected (Tian et al., 2009; Karthik et al., 2019b; Karthik et al., 2019a). This result indicates that there is excess silica in the reaction between bismuth oxynitrate and silica. Therefore, the resulting

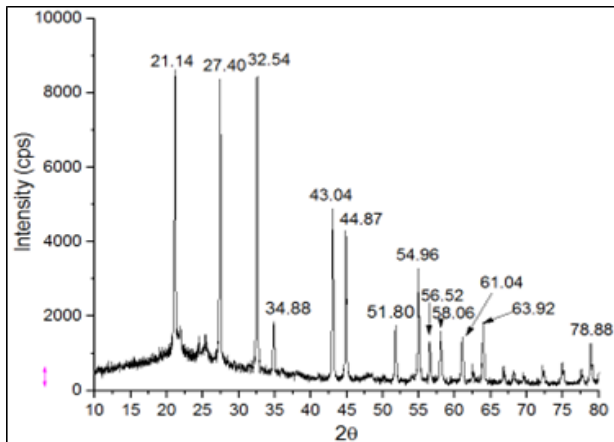
composite can be called a Bi<sub>4</sub>Si<sub>3</sub>O<sub>12</sub>/SiO<sub>2</sub> composite (Chandrawanshi et al., 2020).

**Figure 4.** Elemental Analysis of Binary Metal-Oxide Compounds Bi<sub>4</sub>Si<sub>3</sub>O<sub>12</sub>/SiO<sub>2</sub> Resulting from Analysis using Energy Dispersive X-Ray (EDX)

The reaction mechanism that may occur in the synthesis of bismuth silicate is a complexing reaction between a complex compound of silicon in powdered OPL and bismuth ions in the compound bismuth nitrate. Moreover, by heating at high temperatures, the degradation reaction of the complex compound occurred as well as the reaction process for the formation of

**Table 2.** Elemental Composition of  $\text{Bi}_4\text{Si}_3\text{O}_{12}/\text{SiO}_2$  Resulting from Analysis using Energy Dispersive X-Ray (EDX)

Element	K(eV)	%Mass
C	0.277	13.68
O	0.525	19.05
Al	1.486	0.22
Si	1.739	8.37
Bi	2.419	58.00
Fe	6.398	0.07

**Figure 5.** X-Ray Diffraction Pattern of the Ternary Metal-Oxide  $\text{Bi}_4\text{Si}_3\text{O}_{12}/\text{SiO}_2\text{-TiO}_2$ 

bismuth silicate. Another possibility is that the silicon complex compound in palm leaf powder first degrades into  $\text{SiO}_2$ , as well as bismuth oxynitrate, which turns into  $\text{Bi}_2\text{O}_3$ . These two compounds then interact through a solid-state reaction and produce bismuth silicate. To investigate the morphology and elemental content of the resulting  $\text{Bi}_4\text{Si}_3\text{O}_{12}/\text{SiO}_2$  materials, SEM-EDX analysis was conducted. Figure 3 shows the results of the SEM analysis, and Figure 4 and Table 2 show the results of the EDX analysis.

Figure 3 shows that the morphology of the resulting  $\text{Bi}_4\text{Si}_3\text{O}_{12}/\text{SiO}_2$  material is in the form of an uneven solid that is also interspersed with several detectable pores. As shown in Figure 4 and Table 2, further analysis using SEM-EDX gives the morphology and element content.

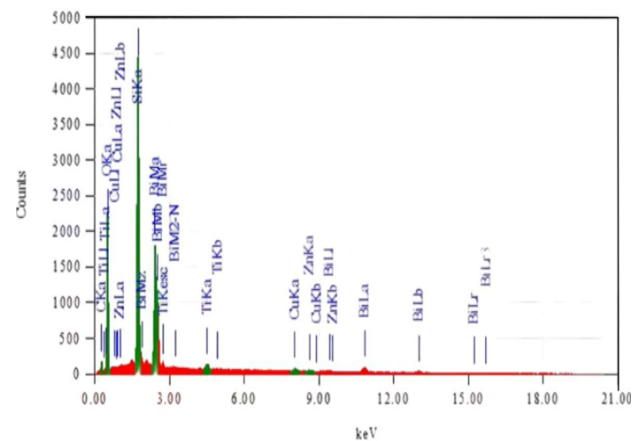
Figure 4 and Table 2 show that the bismuth content is very large, as is the accompanying silica. This indicates that the main composition contained in the sample actually contains bismuth and silica compounds. The research was continued by synthesizing the ternary metal oxide  $\text{Bi}_4\text{Si}_3\text{O}_{12}/\text{SiO}_2\text{-TiO}_2$  by carrying out the reaction between  $\text{TiO}_2$  precursors by adding TTIP. Figure 5 presents the results of the XRD analysis of the synthesized products using TTIP.

Figure 5 shows that the peaks detected mainly indicate the presence of the  $\text{Bi}_4\text{Si}_3\text{O}_{12}$  compound. The  $\text{TiO}_2$  compound, which is expected to be visible in the XRD diffraction, cannot

**Table 3.** Elemental Composition of  $\text{Bi}_4\text{Si}_3\text{O}_{12}/\text{SiO}_2\text{-TiO}_2$  Resulting from Analysis using Energy Dispersive X-Ray (EDX)

Element	K(eV)	% Mass
C	0.277	10.55
O	0.525	35.68
Si	1.739	18.25
Bi	2.419	32.49
Ti	4.508	0.85
Cu	8.040	1.25
Zn	8.630	0.94

be clearly detected. This is mainly because the precursor added to synthesize  $\text{TiO}_2$  is very small compared to the content of  $\text{Bi}_4\text{Si}_3\text{O}_{12}$ . Figure 6, Table 3, and Figure 7 show the titanium content in the sample and the morphology of the resulting compound.

**Figure 6.** Elemental Analysis of Binary Metal-Oxide Compounds  $\text{Bi}_4\text{Si}_3\text{O}_{12}/\text{SiO}_2\text{-TiO}_2$  Resulting from Analysis using Energy Dispersive X-Ray (EDX)

In Figure 6 and Table 3, elemental titanium is detected in the product resulting from the heating of  $\text{Bi}_4\text{Si}_3\text{O}_{12}/\text{SiO}_2$  and TTIP. The presence of this titanium indicates that TTIP has been degraded and further oxidized to  $\text{TiO}_2$  at high temperatures.

Figure 7(a) shows that the ternary metal oxide compound  $\text{Bi}_4\text{Si}_3\text{O}_{12}/\text{TiO}_2\text{-SiO}_2$  undergoes surface changes compared to  $\text{Bi}_4\text{Si}_3\text{O}_{12}/\text{SiO}_2$  itself. This surface change can be caused due to the presence of  $\text{TiO}_2$ , which has been attached to the  $\text{Bi}_4\text{Si}_3\text{O}_{12}/\text{SiO}_2$  solid. As shown in Figure 7(b), the pores of the resulting solid material are more clearly visible compared to the  $\text{Bi}_4\text{Si}_3\text{O}_{12}/\text{SiO}_2$  solid.

Figure 8 shows the presence of several typical peaks that emerge from the  $\text{Bi}_4\text{Si}_3\text{O}_{12}/\text{TiO}_2\text{-SiO}_2$  solid. These peaks are  $3457$ ,  $1632$ ,  $1098$ ,  $795$ ,  $615$ , and  $549\text{ cm}^{-1}$ . The peaks at  $3457$  and  $1632\text{ cm}^{-1}$  show the presence of water molecules adsorbed in the solid. The presence of  $\text{TiO}_2$  causes the typical



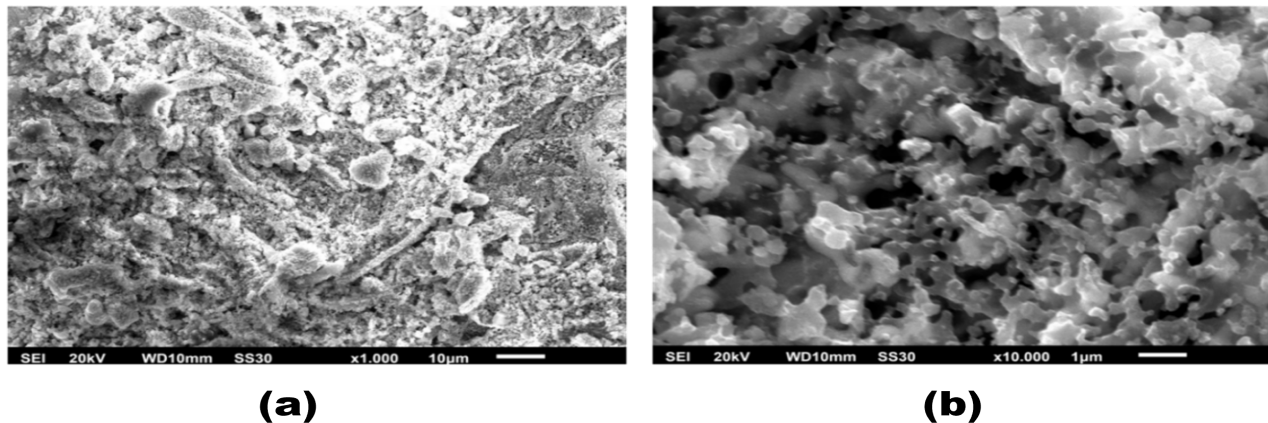


**Figure 7.** SEM Pattern of the as-Prepared  $\text{Bi}_4\text{Si}_3\text{O}_{12}/\text{SiO}_2\text{-TiO}_2$  (a) 1000 $\times$  Magnification; (b) 10000 $\times$  Magnification

peaks for this ternary metal oxide, namely, 1098, 795, 615, and 549  $\text{cm}^{-1}$ .

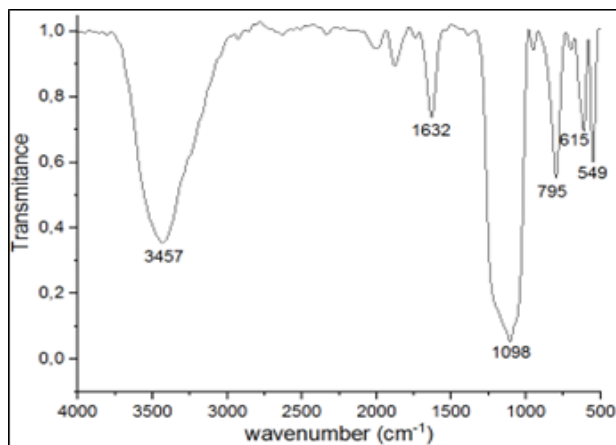


**Figure 8.** FTIR Pattern of the as-Prepared  $\text{Bi}_4\text{Si}_3\text{O}_{12}/\text{SiO}_2\text{-TiO}_2$

#### 4. CONCLUSIONS

The synthesis of bismuth silicate has been successfully carried out by utilizing the in situ reaction between bismuth oxynitrate and powdered OPLs as a source of silica. The reaction product in the form of a solid powder that has been produced can be used to form ternary metal oxide ( $\text{Bi}_4\text{Si}_3\text{O}_{12}/\text{SiO}_2\text{-TiO}_2$ ) by reaction with TTIP as a precursor. The resulting composite has the potential to act as antibacterial and/or catalyst, especially in photocatalytic reactions.

#### 5. ACKNOWLEDGMENT

All authors are very grateful to the Ministry of Education, Culture, Research, and Technology of the Republic of Indonesia for providing funding for this research through the 2022 "Penelitian Dasar" scheme, contract number 013/E5/PG.02.00. PT/2022, March 16th, 2022, between the Institute of Research

and Community Service (LPPM) at Universitas Bengkulu (UNIB) and the Ministry of Education, Culture, Research, and Technology of the Republic of Indonesia, and contract number 733/UN30.15/PP/2022, March 22<sup>nd</sup>, 2022, between the principal investigator and LPPM at the Universitas Bengkulu.

#### REFERENCES

- Arefieva, O., M. Vasilyeva, L. Zemnukhova, D. Opra, D. Nikolaeva, V. Tkachev, and D. Shlyk (2023). Effect of Silica Source on Photocatalytic Properties of  $\text{Bi}_2\text{O}_3/\text{Bi}_2\text{SiO}_5$  Heterostructure. *Journal of Bioresources and Bioproducts*, **8**(2); 176–186
- Back, M., E. Casagrande, E. Trave, D. Cristofori, E. Ambrosi, F. Dallo, M. Roman, J. Ueda, J. Xu, S. Tanabe (2020). Confined-Melting-Assisted Synthesis of Bismuth Silicate Glass-Ceramic Nanoparticles: Formation and Optical Thermometry Investigation. *ACS Applied Materials & Interfaces*, **12**(49); 55195–55204
- Bai, Z., X. Ba, R. Jia, B. Liu, Z. Xiao, and X. Zhang (2007). Preparation and Characterization of Bismuth Silicate Nanopowders. *Frontiers of Chemistry in China*, **2**; 131–134
- Bai, Z., Y. Hu, S. Yan, W. Shan, and C. Wei (2017). Preparation of Mesoporous  $\text{SiO}_2/\text{Bi}_2\text{O}_3/\text{TiO}_2$  Superhydrophilic Thin Films and Their Surface Self-Cleaning Properties. *RSC Advances*, **7**(4); 1966–1974
- Batool, S., Z. Imran, K. Rasool, J. Ambreen, S. Hassan, S. Arif, M. Ahmad, and M. Rafiq (2020). Study of Electric Conduction Mechanisms in Bismuth Silicate Nanofibers. *Scientific Reports*, **10**(1); 2775
- Belik, Y., T. Kharlamova, A. Vodyankin, V. Svetlichnyi, and O. Vodyankina (2020). Mechanical Activation for Soft Synthesis of Bismuth Silicates. *Ceramics International*, **46**(8); 10797–10806
- Bilecka, I., I. Djerdj, and M. Niederberger (2008). One-Minute Synthesis of Crystalline Binary and Ternary Metal Oxide Nanoparticles. *Chemical Communications*, (7); 886–888
- Chandrawanshi, E., D. Bisen, N. Brahme, G. Banjare, T. Rich-

- hariya, and Y. Patle (2020). Photoluminescence and Comparative Thermoluminescence Studies of UV/ $\gamma$ -Irradiated Dy<sup>3+</sup> Doped Bismuth Silicate Phosphor. *Journal of Materials Science: Materials in Electronics*, **31**; 14454–14465
- Gadea, C., N. Phatharapeetranun, B. Ksapabutr, J.-C. Grivel, and V. Esposito (2018). Stoichiometric Control in Bi<sub>4</sub>Ti<sub>3</sub>O<sub>12</sub> Synthesis by Novel Hybrid Solid State Reaction. *Materials Letters*, **221**; 101–103
- Jia, K. L., J. Qu, S. M. Hao, F. An, Y. Q. Jing, and Z. Z. Yu (2017). One-Pot Synthesis of Bismuth Silicate Heterostructures with Tunable Morphology and Excellent Visible Light Photodegradation Performances. *Journal of Colloid and Interface Science*, **506**; 255–262
- Karthik, K., K. S. Devi, D. Pinheiro, and S. Sugunan (2019a). Photocatalytic Activity of Bismuth Silicate Heterostructures Synthesized Via Surfactant Mediated Sol-Gel Method. *Materials Science in Semiconductor Processing*, **102**; 104589
- Karthik, K., S. D. KR, and D. Pinheiro (2019b). Synthesis of Bismuth Silicate Nanostructures with Tunable Morphology and Enhanced Photocatalytic Activity. *Indian Journal of Chemical Technology*, **26**(2); 170–174
- Khodadoost, S., A. Hadi, J. Karimi-Sabet, M. Mehdipourghazi, and A. Golzary (2017). Optimization of Hydrothermal Synthesis of Bismuth Titanate Nanoparticles and Application for Photocatalytic Degradation of Tetracycline. *Journal of Environmental Chemical Engineering*, **5**(6); 5369–5380
- Kurc, B., K. Siwińska-Stefańska, and T. Jesionowski (2018). Bismuth-Titanium-Silicon-Based Ternary Oxide System: A Comprehensive Analysis and Electrochemical Utility. *Solid State Ionics*, **324**; 92–102
- Lu, J., X. Wang, H. Jiang, and Y. Xu (2013). Synthesis of Bismuth Silicate Powders by Molten Salt Method. *Materials and Manufacturing Processes*, **28**(2); 126–129
- Mao, Y., T.-J. Park, and S. S. Wong (2005). Synthesis of Classes of Ternary Metal Oxide Nanostructures. *Chemical Communications*, (46); 5721–5735
- Marela, S., N. Aini, A. Hardian, V. Suendo, and A. Prasetyo (2021). The Effect of Temperature Synthesis on the Plate-Like Particle of Bi<sub>4</sub>Ti<sub>3</sub>O<sub>12</sub> Obtained by Single Molten NaCl Salt. *The Journal of Pure and Applied Chemistry Research*, **10**(1); 64–71
- Ren, C., W. Qiu, H. Zhang, Z. He, and Y. Chen (2015). Degradation of Benzene on TiO<sub>2</sub>/SiO<sub>2</sub>/Bi<sub>2</sub>O<sub>3</sub> Photocatalysts Under UV and Visible Light. *Journal of Molecular Catalysis A: Chemical*, **398**; 215–222
- Shabalina, A. V., E. Y. Gotovtseva, Y. A. Belik, S. M. Kuzmin, T. S. Kharlamova, S. A. Kulinich, V. A. Svetlichnyi, and O. V. Vodyankina (2022). Electrochemical Study of Semiconductor Properties for Bismuth Silicate-Based Photocatalysts Obtained via Hydro-/Solvothermal Approach. *Materials*, **15**(12); 4099
- Slavov, S. S. and Y. B. Dimitriev (2016). Glass Formation in the E System Bi<sub>2</sub>O<sub>3</sub>-TiO<sub>2</sub>-SiO<sub>2</sub>. *Journal of Chemical Technology & Metallurgy*, **51**(5); 536–546
- Thiruramanathan, P., S. K. Sharma, S. Sankar, R. Sankar Ganesh, A. Marikani, and D. Y. Kim (2016). Synthesis of Bismuth Titanate (BTO) Nanopowder and Fabrication of Microstrip Rectangular Patch Antenna. *Applied Physics A*, **122**; 1–10
- Tian, Q., X. Wang, C. Yu, H. Jiang, Z. Zhang, Y. Wang, and S. Lin (2009). Domain Structure and Defects of Highly Ordered Bi<sub>4</sub>Si<sub>3</sub>O<sub>12</sub> Micro-Crystals. *Science in China Series E: Technological Sciences*, **52**; 2295–2301
- Wang, R. and J. Wu (2017). Structure and Basic Properties of Ternary Metal Oxides and Their Prospects for Application in Supercapacitors. In *Metal Oxides in Supercapacitors*. Elsevier; 99–132
- Zaccariello, G., M. Back, A. Benedetti, P. Canton, E. Cattaruzza, H. Onoda, A. Glisenti, A. Alimonti, B. Bocca, and P. Riello (2019). Bismuth Titanate-Based UV Filters Embedded Mesoporous Silica Nanoparticles: Role of Bismuth Concentration in the Self-Sealing Process. *Journal of Colloid and Interface Science*, **549**; 1–8
- Zaccariello, G., M. Back, M. Zanello, P. Canton, E. Cattaruzza, P. Riello, A. Alimonti, and A. Benedetti (2017). Formation and Controlled Growth of Bismuth Titanate Phases Into Mesoporous Silica Nanoparticles: An Efficient Self-Sealing Nanosystem for UV Filtering in Cosmetic Formulation. *ACS Applied Materials & Interfaces*, **9**(2); 1913–1921